# Supplement for: Deposition, recycling and archival of nitrate stable isotopes between the air-snow interface: comparison between Dronning Maud Land and Dome C, Antarctica

V. Holly L. Winton[1], Alison Ming[1], Nicolas Caillon[2], Lisa Hauge[1], Anna E. Jones[1], Joel Savarino[2], Xin Yang[1], Markus M. Frey[1]

[1]British Antarctic Survey, Cambridge, CB3 0ET, UK
[2]University of Grenoble Alpes, CNRS, IRD, Grenoble INP, IGE, F-38000 Grenoble, France

*Correspondence to*: V. Holly L Winton (vicwin@bas.ac.uk)

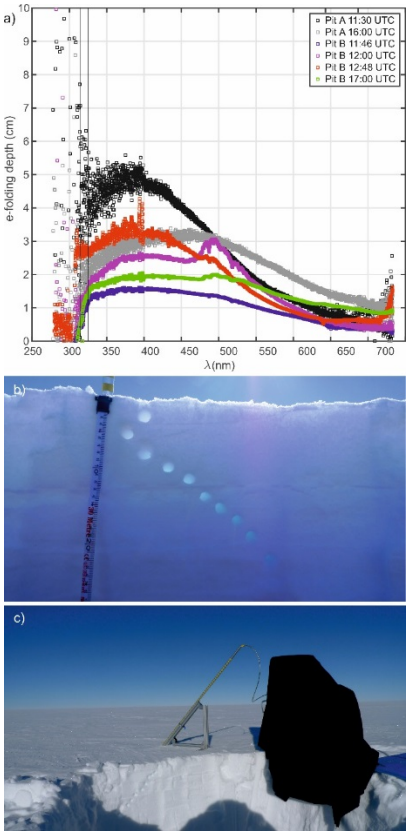


**Figure S1: a) Shown are e-folding depths as a function of wavelength at two locations at Dronning Maud Land (DML; Pit A and B). Times in UTC indicate the median time of the experiment. The vertical solid lines mark the 315-325 nm range, where photolysis rate coefficients of NO3- have their maximum (e.g. Fig. 5b in Frey et al. (2009). b) Frontal view of a snow pit side wall showing pre-cored horizontal holes in the top 27 cm of surface snow pack, where the fibre optics probe was inserted horizontally to measure down-welling irradiance. c) Snow surface with a metal frame on top to keep the fibre optics probe at a 45° angle while it is pushed gradually into the snow pack to measure down-welling irradiance as a function of snow depth. The black cloth covers the spectrometer and a field laptop.**

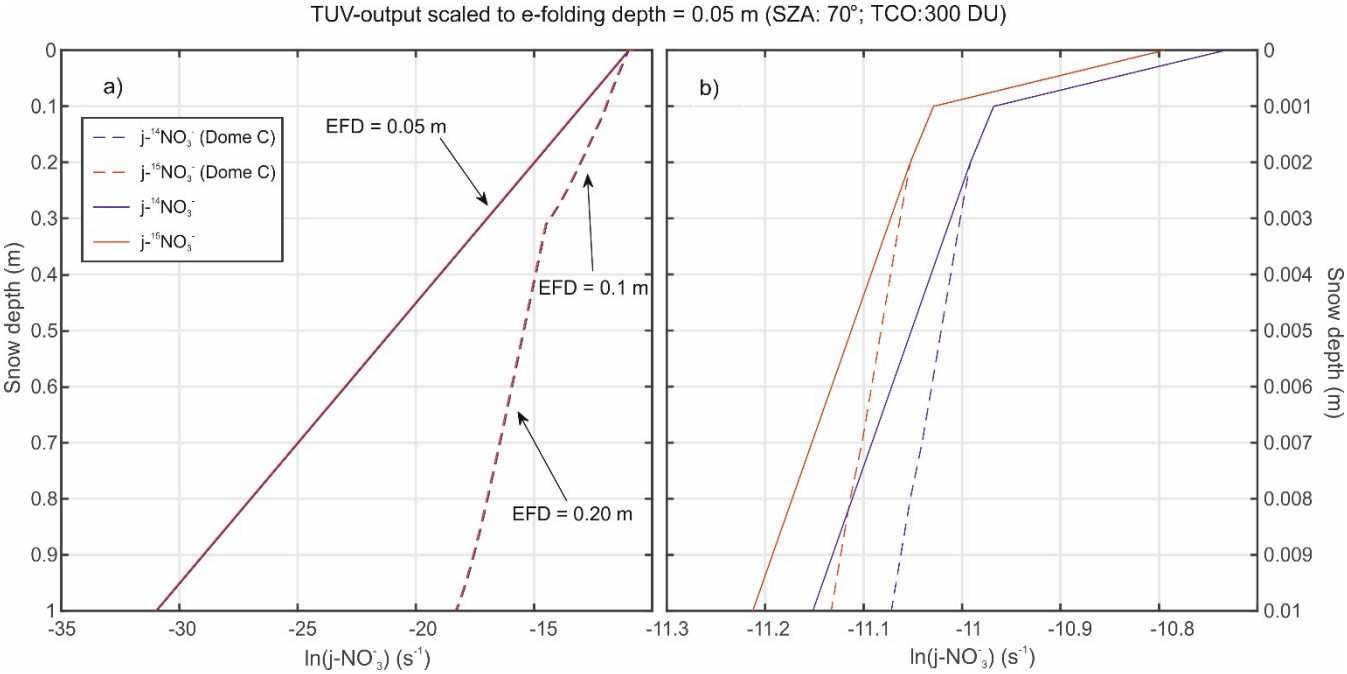


**Figure S2: Modelled J($^{14/15}NO_3^-$) profiles in snow: base case at Dome C (dashed lines) and profiles scaled with a various e-folding depths; shown as an example is the J($^{14/15}NO_3^-$) profile at solar zenith angle (SZA) = 70º and total column ozone (TCO) = 300 DU typical for January at 75º S on the East Antarctic Plateau. EDF: e-folding depth.**

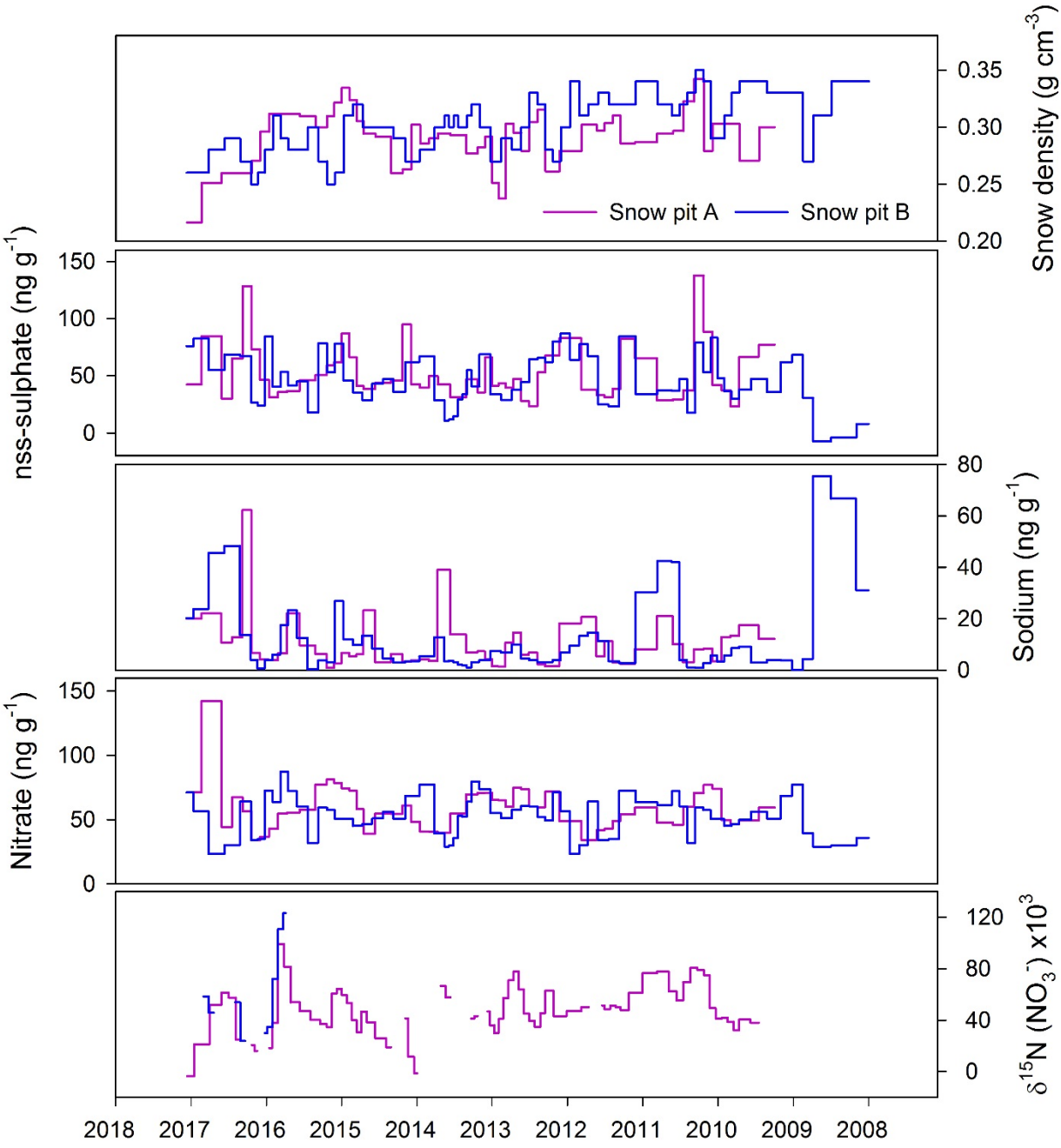


**Figure S3: Dated snow pit profiles of nitrate, sodium, and non sea salt (nss)-sulphate concentration and $\delta^{15}N\text{-}NO_3^-$ at Dronning Maud Land (DML).**

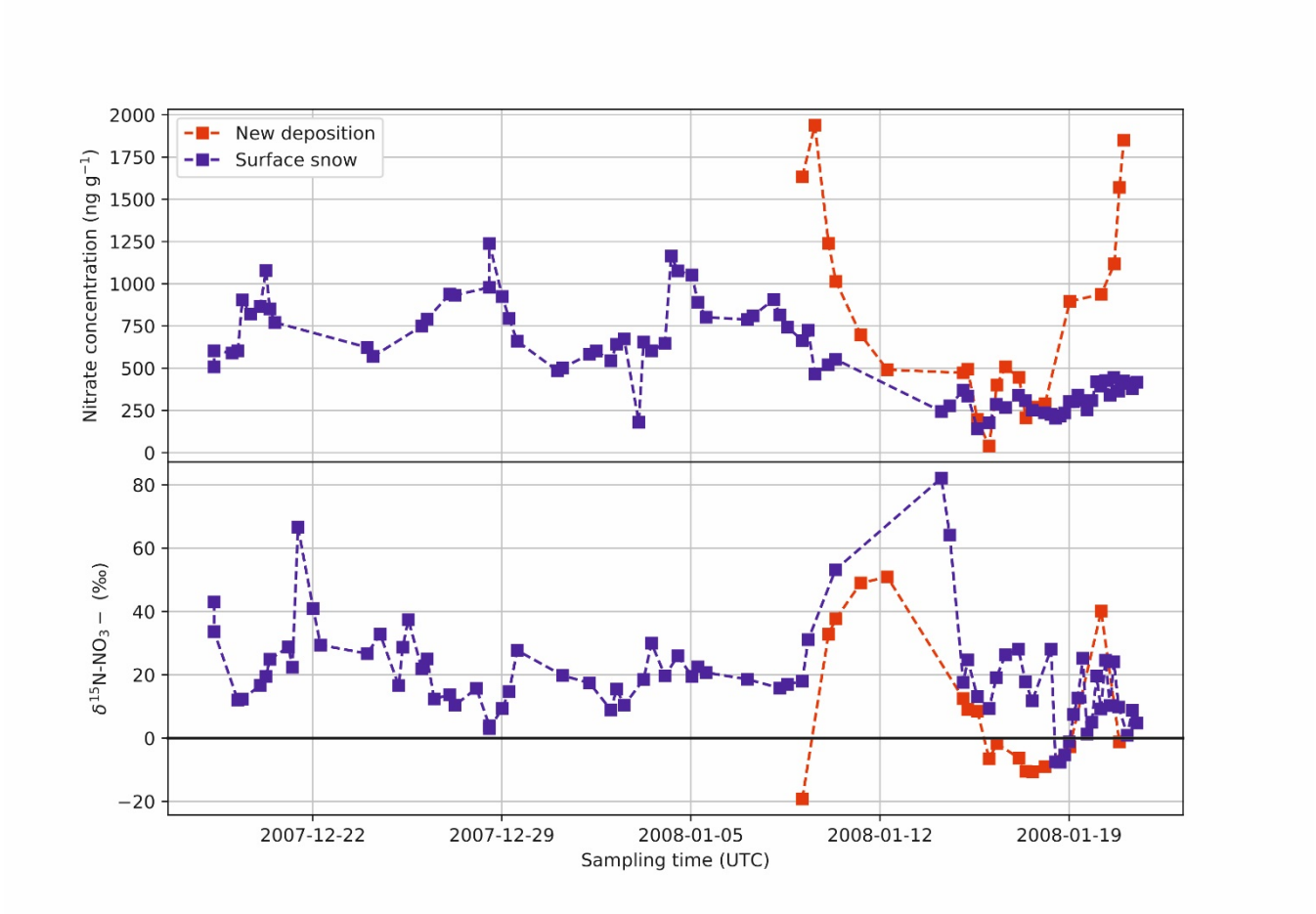


**Figure S4: Nitrate concentration and $\delta^{15}$N-$NO_3^-$ composition in new deposition (diamond dust and hoar frost) and skin layer at Dome C during austral summer in 2007.**

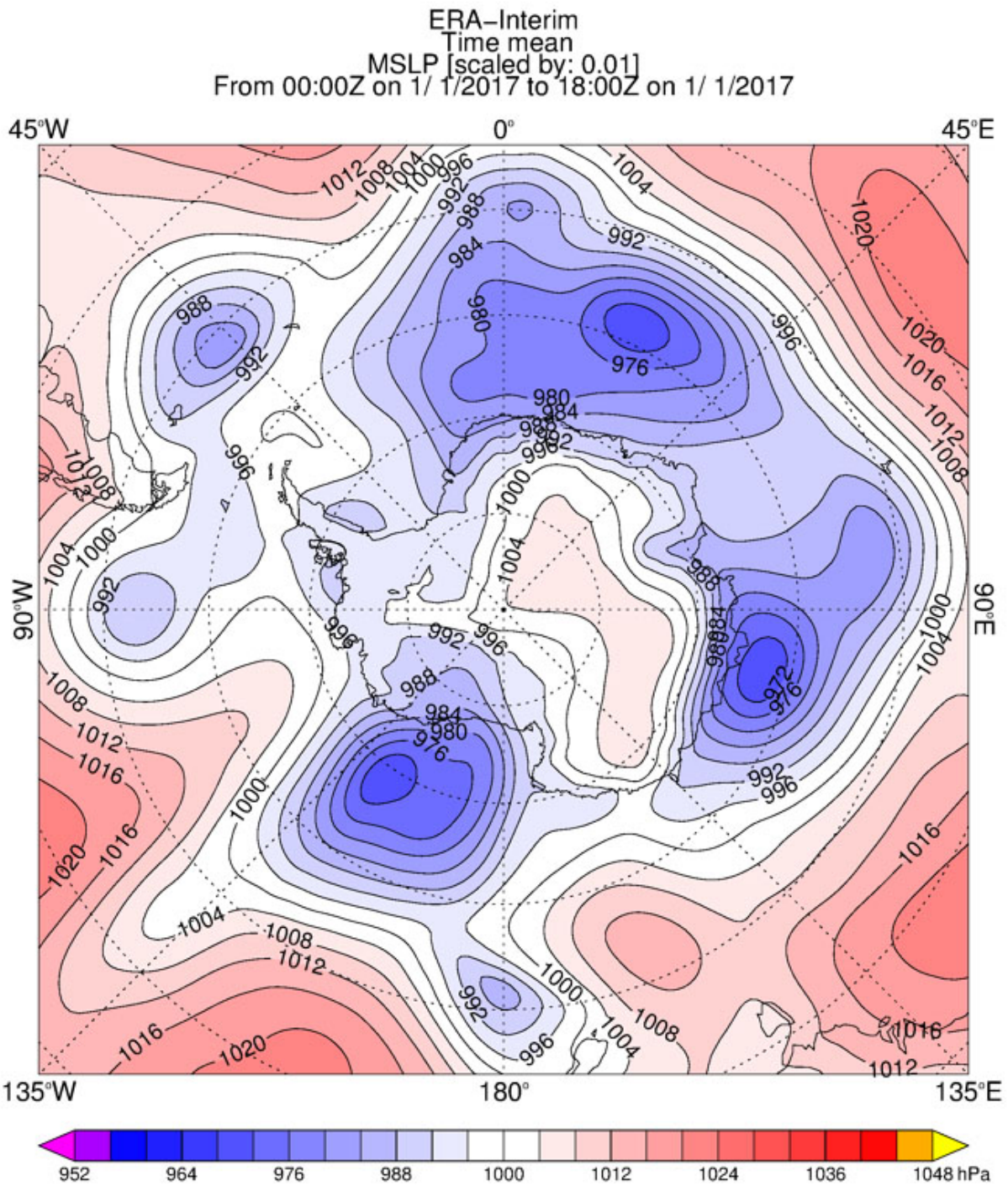


**Figure S5: The surface pressure for 1 January 2017. This day had the largest precipitation event of the month with 0.27 mm. Data source: ERA-interim (https://www.ecmwf.int/en/forecasts/datasets/reanalysis-datasets/era-interim).**

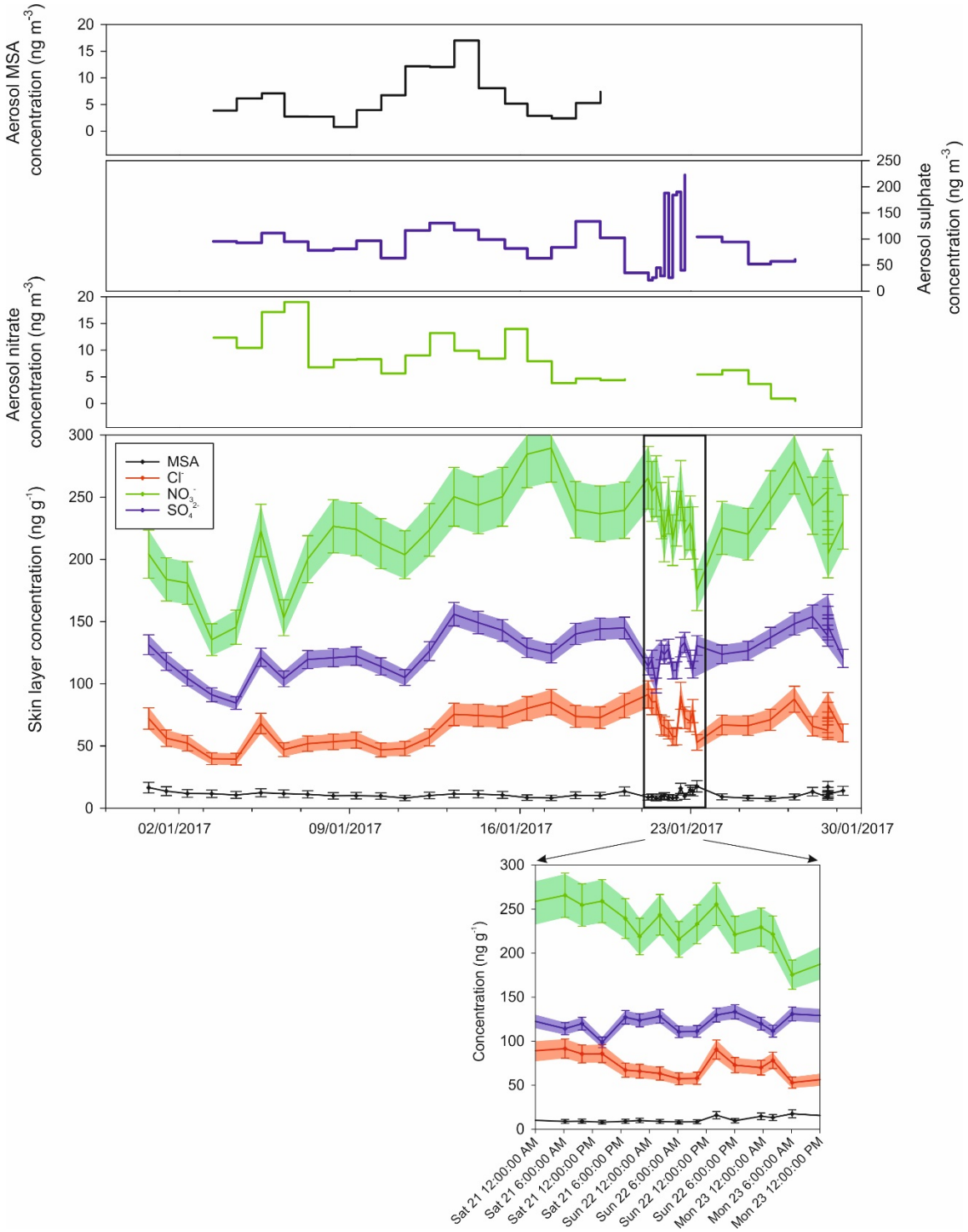


30

**Figure S6: Daily aerosol and skin layer ion mass concentrations at Dronning Maud Land (DML) for the month of January 2017. The shaded area of the skin layer mass concentrations reflects the spatial variability within 2500 $m^2$ area at the site.**

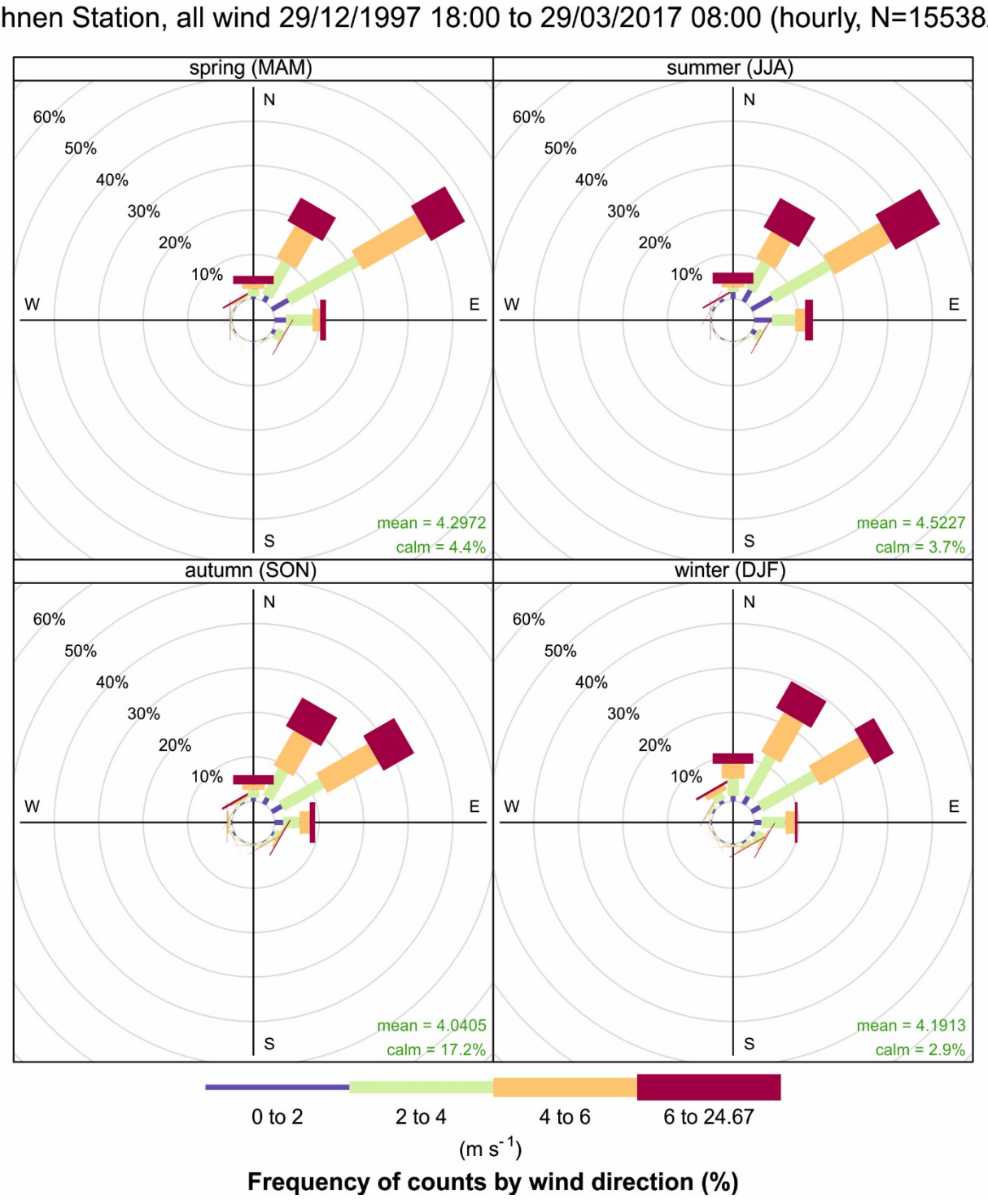


**Figure S7: Seasonal wind rose at Kohnen Station. Data source: Utrecht University automatic weather Station. Wind roses were made using the openair package in R following Carslaw and Ropkins (2012);Carslaw (2014).**

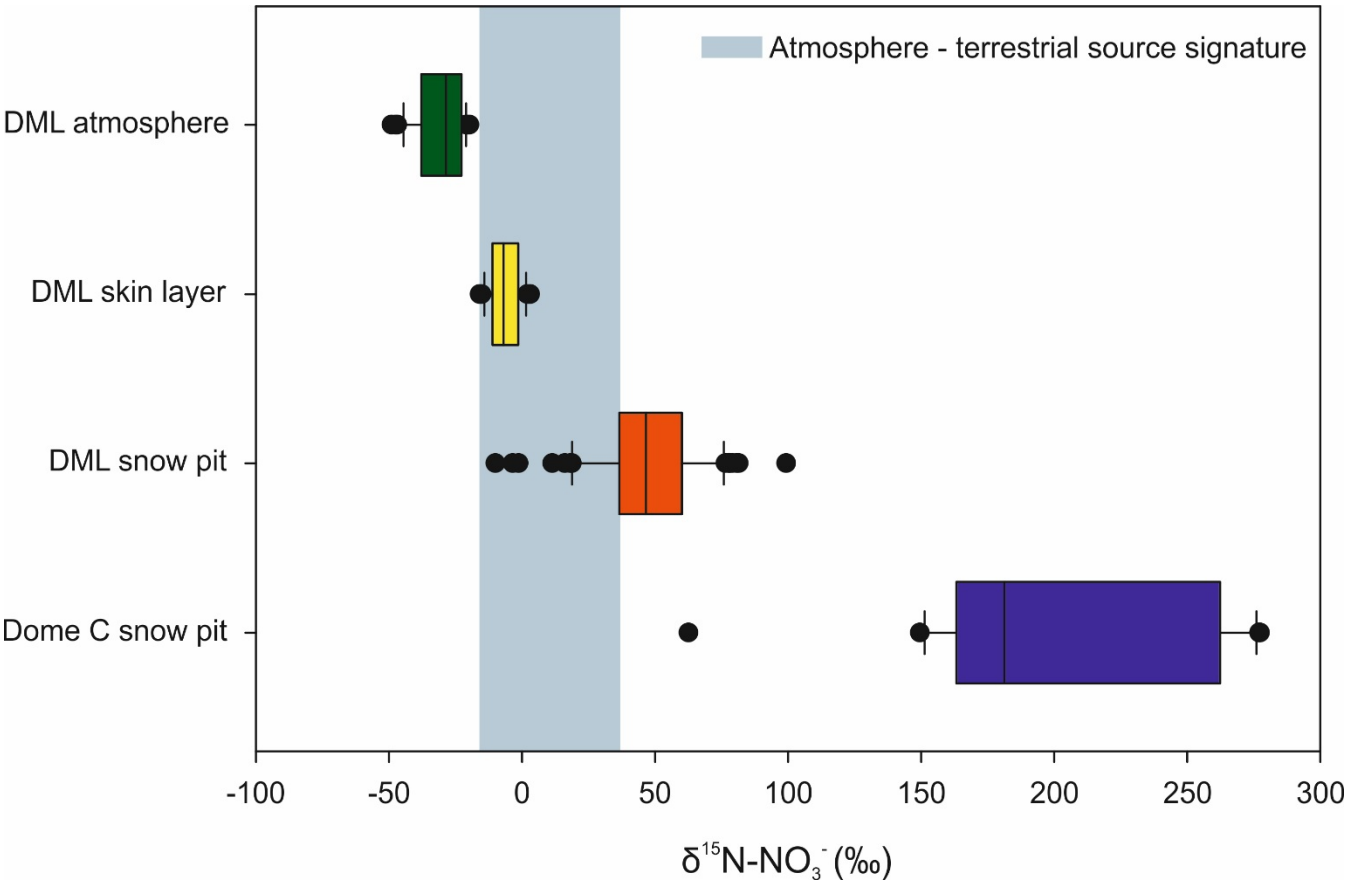


**Figure S8: Box and whisker plot comparing the atmospheric and terrestrial $\delta^{15}N\text{-}NO_3^-$ source signature to Dronning Maud Land (DML) atmospheric, skin layer, snow pit, and Dome C snow pit $\delta^{15}N\text{-}NO_3^-$ signatures. Dome C data source: Frey et al. (2009).**

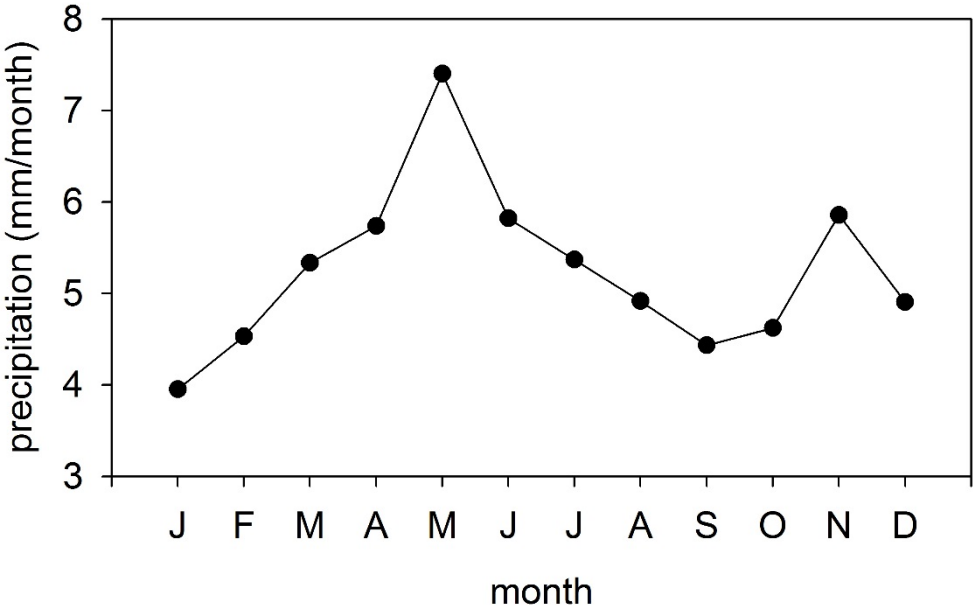


**Figure S9: Seasonal distribution of snowfall at Dronning Maud Land (DML), which has a bimodal distribution with the greatest accumulation in austral autumn and early austral summer. Data source: ERA Interim data, with monthly averages derived from 1980 to 2018 (https://www.ecmwf.int/en/forecasts/datasets/reanalysis-datasets/era-interim).**

**Table S1: Nitrate blank mass concentrations for exposure blank, procedural blank and laboratory blank and detection limits. n: number of blanks.**

| **Snow pit** | **n** | **$NO_3^-$ mass concentration (ng $g^{-1}$)** | **±** |
|---|---|---|---|
| Instrumental blank | 12 | 0.7 | 0.2 |
| Exposure blank (Corning tubes) | 12 | 6 | 3.0 |
| Limit of detection (LOD) | 7 | 3 | |
| **Surface snow** | **n** | **$NO_3^-$ mass concentration (ng $g^{-1}$)** | **±** |
| Instrumental blank | 15 | 5 | 1.2 |
| Exposure blank (Whirl-pak® bags) | 5 | 4 | 1.0 |
| Limit of detection (LOD) | 10 | 1 | |
| **Aerosol** | **n** | **$NO_3^-$ mass concentration (ng $g^{-1}$)** | **±** |
| Laboratory blank | 3 | 3 | 2.0 |
| Procedure blank | 4 | 280 | 78.9 |
| Exposure blank | 2 | 330 | 49.2 |
| Limit of detection (LOD) | 3 | 3 | |

**Table S2: e-folding depths calculated from irradiance profiles in the surface snow pack at two locations (pit A and B; same locations as snow pit A and B respectively) at Dronning Maud Land (DML). Reported are mean and standard deviation of e-folding depth in the 315-325 nm range, where the photolysis rate coefficients of $NO_3^-$ have their maximum.**

| Pit | Sampled depth range (cm) | Time of experiment (UTC) | Method | e-folding depth (± 1 σ, cm) |
|---|---|---|---|---|
| Pit A | 0-22 | 27/01/2017 11:30 | Horizontal | 4.0 ± 1.3 |
| Pit A | 0-12 | 27/01/2017 16:00 | Horizontal | 1.9 ± 0.5 |
| Pit B | 0-29 | 28/01/2017 11:46 | Horizontal | 0.9 ± 0.3 |
| Pit B | 0-29 | 28/01/2017 12:00 | Horizontal | 1.3 ± 0.1 |
| Pit B | 0-41 | 28/01/2017 12:48 | º45 | 2.7 ± 0.1 |
| Pit B | 0-21 | 28/01/2017 17:00 | º45 | 1.1 ± 0.4 |

**Table S3: Input parameters for TRANSITS modelling at Dronning Maud Land (DML).**

| Time step (weeks) | Accumulation repartition (fraction) | [1]Atmospheric $NO_3^-$ mass concentration (ng $m^{-3}$) | Atmospheric boundary layer height (m) | [2]Air temperature (K) | [2]Air pressure (mbar) | Ground level ozone (ppbv) | $D^{17}O$ of ozone (‰) | Exported fraction (fraction) | Stratospheric flux repartition (fraction) | Stratospheric $\delta^{15}N$-$NO_3^-$ (‰) | Stratospheric $D^{17}O$ (‰) | Long distance repartition (fraction) | Long distance $\delta^{15}N$-$NO_3^-$ (‰) | Long distance D17O (‰) | [3]Ozone column (Dobson units) | Mean solar zenith angle (°) |
|---|---|---|---|---|---|---|---|---|---|---|---|---|---|---|---|---|
| 0 | 0.019 | 8.93 | 50 | 247.9 | 681.3 | 32.9 | 25.2 | 0.2 | 0.067 | 19 | 42 | 0.019 | 0 | 30 | 306 | 112.9 |
| 1 | 0.019 | 8.87 | 50 | 251.6 | 684.5 | 34.0 | 25.2 | 0.2 | 0.067 | 19 | 42 | 0.019 | 0 | 30 | 298 | 112.6 |
| 2 | 0.019 | 9.40 | 50 | 247.4 | 677.4 | 34.5 | 25.2 | 0.2 | 0.067 | 19 | 42 | 0.019 | 0 | 30 | 294 | 112.0 |
| 3 | 0.019 | 10.40 | 50 | 242.9 | 676.5 | 35.1 | 25.2 | 0.2 | 0.067 | 19 | 42 | 0.019 | 0 | 30 | 284 | 111.0 |
| 4 | 0.019 | 11.17 | 50 | 249.0 | 676.1 | 34.9 | 25.2 | 0.2 | 0.067 | 19 | 42 | 0.019 | 0 | 30 | 269 | 109.8 |
| 5 | 0.019 | 11.15 | 50 | 250.6 | 679.9 | 35.0 | 25.2 | 0.2 | 0.067 | 19 | 42 | 0.019 | 0 | 30 | 256 | 108.2 |
| 6 | 0.019 | 10.29 | 50 | 250.9 | 684.1 | 34.0 | 25.2 | 0.2 | 0.067 | 19 | 42 | 0.019 | 0 | 30 | 243 | 106.5 |
| 7 | 0.019 | 9.59 | 50 | 249.8 | 684.2 | 34.3 | 25.2 | 0.2 | 0.067 | 19 | 42 | 0.019 | 0 | 30 | 221 | 104.5 |
| 8 | 0.019 | 9.25 | 50 | 250.6 | 680.2 | 32.1 | 25.2 | 0.2 | 0.067 | 19 | 42 | 0.019 | 0 | 30 | 211 | 102.3 |
| 9 | 0.019 | 11.07 | 50 | 249.6 | 681.2 | 33.8 | 25.2 | 0.2 | 0.067 | 19 | 42 | 0.019 | 0 | 30 | 189 | 100.0 |
| 10 | 0.019 | 13.99 | 50 | 247.1 | 677.7 | 33.8 | 25.2 | 0.2 | 0.067 | 19 | 42 | 0.019 | 0 | 30 | 166 | 97.5 |
| 11 | 0.019 | 18.93 | 50 | 251.0 | 681.8 | 33.0 | 25.2 | 0.2 | 0.067 | 19 | 42 | 0.019 | 0 | 30 | 146 | 94.9 |
| 12 | 0.019 | 24.77 | 50 | 239.8 | 664.2 | 32.2 | 25.2 | 0.2 | 0.050 | 19 | 42 | 0.019 | 0 | 30 | 137 | 92.3 |
| 13 | 0.019 | 30.61 | 50 | 222.3 | 674.0 | 31.7 | 25.2 | 0.2 | 0.033 | 19 | 42 | 0.019 | 0 | 30 | 131 | 89.6 |
| 14 | 0.019 | 34.82 | 50 | 239.2 | 684.2 | 30.7 | 25.2 | 0.2 | 0.017 | 19 | 42 | 0.019 | 0 | 30 | 136 | 86.9 |
| 15 | 0.019 | 38.25 | 50 | 242.9 | 676.9 | 30.4 | 25.2 | 0.2 | 0.000 | 19 | 42 | 0.019 | 0 | 30 | 146 | 84.3 |
| 16 | 0.019 | 39.25 | 50 | 238.9 | 676.4 | 29.2 | 25.2 | 0.2 | 0.000 | 19 | 42 | 0.019 | 0 | 30 | 158 | 81.7 |
| 17 | 0.019 | 39.77 | 50 | 245.1 | 661.5 | 28.2 | 25.2 | 0.2 | 0.000 | 19 | 42 | 0.019 | 0 | 30 | 180 | 79.2 |
| 18 | 0.019 | 39.77 | 50 | 245.3 | 665.9 | 27.9 | 25.2 | 0.2 | 0.000 | 19 | 42 | 0.019 | 0 | 30 | 199 | 76.8 |
| 19 | 0.019 | 42.20 | 50 | 232.2 | 666.1 | 29.0 | 25.2 | 0.2 | 0.000 | 19 | 42 | 0.019 | 0 | 30 | 213 | 74.6 |
| 20 | 0.019 | 43.95 | 50 | 233.4 | 672.5 | 32.2 | 25.2 | 0.2 | 0.000 | 19 | 42 | 0.019 | 0 | 30 | 229 | 72.6 |
| 21 | 0.019 | 46.44 | 50 | 228.5 | 681.6 | 35.5 | 25.2 | 0.2 | 0.000 | 19 | 42 | 0.019 | 0 | 30 | 243 | 70.9 |
| 22 | 0.019 | 47.82 | 50 | 238.3 | 666.9 | 32.2 | 25.2 | 0.2 | 0.000 | 19 | 42 | 0.019 | 0 | 30 | 257 | 69.5 |
| 23 | 0.019 | 47.40 | 50 | 228.0 | 649.1 | 33.1 | 25.2 | 0.2 | 0.000 | 19 | 42 | 0.019 | 0 | 30 | 272 | 68.3 |
| 24 | 0.019 | 44.66 | 50 | 246.8 | 677.8 | 31.4 | 25.2 | 0.2 | 0.000 | 19 | 42 | 0.019 | 0 | 30 | 281 | 67.5 |
| 25 | 0.019 | 41.45 | 50 | 247.5 | 678.1 | 32.4 | 25.2 | 0.2 | 0.000 | 19 | 42 | 0.019 | 0 | 30 | 284 | 67.1 |
| 26 | 0.019 | 37.43 | 50 | 241.4 | 666.8 | 26.1 | 25.2 | 0.2 | 0.000 | 19 | 42 | 0.019 | 0 | 30 | 281 | 67.1 |

| | | | | | | | | | | | | | | | | |
|---|---|---|---|---|---|---|---|---|---|---|---|---|---|---|---|---|
| 27 | 0.019 | 34.15 | 50 | 241.0 | 673.8 | 29.1 | 25.2 | 0.2 | 0.000 | 19 | 42 | 0.019 | 0 | 30 | 275 | 68.1 |
| 28 | 0.019 | 31.44 | 50 | 244.4 | 680.3 | 26.0 | 25.2 | 0.2 | 0.000 | 19 | 42 | 0.019 | 0 | 30 | 276 | 69.1 |
| 29 | 0.019 | 30.86 | 50 | 241.6 | 669.0 | 17.7 | 25.2 | 0.2 | 0.000 | 19 | 42 | 0.019 | 0 | 30 | 273 | 70.5 |
| 30 | 0.019 | 30.18 | 50 | 245.9 | 673.4 | 22.7 | 25.2 | 0.2 | 0.000 | 19 | 42 | 0.019 | 0 | 30 | 269 | 72.2 |
| 31 | 0.019 | 30.25 | 50 | 243.3 | 677.7 | 25.4 | 25.2 | 0.2 | 0.000 | 19 | 42 | 0.019 | 0 | 30 | 267 | 74.1 |
| 32 | 0.019 | 29.37 | 50 | 244.9 | 677.6 | 21.0 | 25.2 | 0.2 | 0.000 | 19 | 42 | 0.019 | 0 | 30 | 259 | 76.3 |
| 33 | 0.019 | 27.66 | 50 | 242.3 | 677.1 | 21.6 | 25.2 | 0.2 | 0.000 | 19 | 42 | 0.019 | 0 | 30 | 260 | 78.7 |
| 34 | 0.019 | 24.76 | 50 | 240.6 | 678.1 | 20.9 | 25.2 | 0.2 | 0.000 | 19 | 42 | 0.019 | 0 | 30 | 259 | 81.2 |
| 35 | 0.019 | 21.71 | 50 | 240.5 | 677.2 | 20.4 | 25.2 | 0.2 | 0.000 | 19 | 42 | 0.019 | 0 | 30 | 257 | 83.8 |
| 36 | 0.019 | 18.77 | 50 | 241.0 | 676.4 | 19.4 | 25.2 | 0.2 | 0.000 | 19 | 42 | 0.019 | 0 | 30 | 253 | 86.5 |
| 37 | 0.019 | 16.45 | 50 | 239.2 | 680.1 | 20.2 | 25.2 | 0.2 | 0.000 | 19 | 42 | 0.019 | 0 | 30 | 252 | 89.2 |
| 38 | 0.019 | 14.60 | 50 | 241.0 | 677.7 | 21.5 | 25.2 | 0.2 | 0.000 | 19 | 42 | 0.019 | 0 | 30 | 253 | 91.9 |
| 39 | 0.019 | 13.59 | 50 | 240.8 | 672.3 | 21.1 | 25.2 | 0.2 | 0.000 | 19 | 42 | 0.019 | 0 | 30 | 254 | 94.6 |
| 40 | 0.019 | 12.46 | 50 | 237.9 | 679.4 | 22.5 | 25.2 | 0.2 | 0.000 | 19 | 42 | 0.019 | 0 | 30 | 253 | 97.2 |
| 41 | 0.019 | 11.47 | 50 | 242.2 | 680.8 | 24.4 | 25.2 | 0.2 | 0.000 | 19 | 42 | 0.019 | 0 | 30 | 258 | 99.7 |
| 42 | 0.019 | 9.81 | 50 | 230.1 | 677.9 | 25.2 | 25.2 | 0.2 | 0.000 | 19 | 42 | 0.019 | 0 | 30 | 267 | 102.1 |
| 43 | 0.019 | 8.11 | 50 | 234.1 | 662.8 | 25.7 | 25.2 | 0.2 | 0.000 | 19 | 42 | 0.019 | 0 | 30 | 279 | 104.3 |
| 44 | 0.019 | 6.51 | 50 | 241.7 | 673.2 | 27.5 | 25.2 | 0.2 | 0.000 | 19 | 42 | 0.019 | 0 | 30 | 281 | 106.3 |
| 45 | 0.019 | 5.77 | 50 | 242.7 | 673.5 | 29.0 | 25.2 | 0.2 | 0.000 | 19 | 42 | 0.019 | 0 | 30 | 290 | 108.1 |
| 46 | 0.019 | 5.70 | 50 | 240.1 | 676.0 | 29.6 | 25.2 | 0.2 | 0.000 | 19 | 42 | 0.019 | 0 | 30 | 288 | 109.7 |
| 47 | 0.019 | 6.84 | 50 | 237.0 | 674.7 | 30.8 | 25.2 | 0.2 | 0.000 | 19 | 42 | 0.019 | 0 | 30 | 291 | 111.0 |
| 48 | 0.019 | 8.03 | 50 | 238.1 | 671.2 | 31.2 | 25.2 | 0.2 | 0.000 | 19 | 42 | 0.019 | 0 | 30 | 297 | 111.9 |
| 49 | 0.019 | 9.11 | 50 | 235.1 | 664.7 | 32.1 | 25.2 | 0.2 | 0.017 | 19 | 42 | 0.019 | 0 | 30 | 301 | 112.6 |
| 50 | 0.019 | 9.53 | 50 | 236.3 | 667.1 | 32.6 | 25.2 | 0.2 | 0.033 | 19 | 42 | 0.019 | 0 | 30 | 303 | 112.9 |
| 51 | 0.019 | 9.26 | 50 | 240.7 | 674.4 | 33.6 | 25.2 | 0.2 | 0.050 | 19 | 42 | 0.019 | 0 | 30 | 304 | 112.9 |

[1]Weller and Wagenbach (2007)

[2]Utrecht University automatic weather Station (AWS) at DML05/Kohnen (AWS9; https://www.projects.science.uu.nl/iceclimate/aws/files_oper/oper_20632).

[3]NIWA Bodeker combined dataset version 3.3 at the location of the snow pit site averaged from 2000 to 2016 (http://www.bodekerscientific.com/data/total-column-ozone).

**Table S4: Average photolysis rate coefficients of nitrate in snow above the East Antarctic Plateau observed at SZA = 68º compared to model estimates from TUV-snow. DML: Dronning Maud Land.**

| Location | TCO (DU) | $2\pi$ J($NO_3^-$) ($s^{-1}$) | Period of observations |
|---|---|---|---|
| [1]DML | 306 | 0.98 $x10^{-8}$ | 1-14 January 2017 |
| [2]Dome C | 287 | 2.52 $x10^{-8}$ | 1-14 January 2012 |
| [3]TUV-snow | 275 | 2.71 $x10^{-8}$ | |
| [3]TUV-snow | 300 | 2.57 $x10^{-8}$ | |
| [3]TUV-snow | 325 | 2.44 $x10^{-8}$ | |

[1]This study

[2]Kukui et al. (2013)

[3]Erbland et al. (2015)

**Table S5: Atmospheric nitrate mass concentration and dry deposition fluxes over the ISOL-ICE campaign at Kohnen Station, Dronning Maud Land (DML). No data: n.d.**

| Sample name | Start time | End time | *Corrected volume ($m^3$) | $NO_3^-$ mass concentration (ng $m^{-3}$) | $NO_3^-$ dry deposition flux (pg $m^{-2}$ $s^{-1}$) |
|---|---|---|---|---|---|
| Kohnen16-17_N_01 | 03/01/2017 09:33 | 04/01/2017 08:07 | 1651 | 12 | 99 |
| Kohnen16-17_N_02 | 04/01/2017 08:28 | 05/01/2017 08:33 | 1815 | 10 | 84 |
| Kohnen16-17_N_03 | 05/01/2017 09:14 | 06/01/2017 07:09 | 1613 | 17 | 137 |
| Kohnen16-17_N_04 | 06/01/2017 07:29 | 07/01/2017 06:34 | 1719 | 19 | 152 |
| Kohnen16-17_N_05 | 07/01/2017 06:55 | 08/01/2017 07:37 | 1872 | 7 | 54 |
| Kohnen16-17_N_06 | 08/01/2017 07:56 | 09/01/2017 06:24 | 1661 | 8 | 66 |
| Kohnen16-17_N_07 | 09/01/2017 06:40 | 10/01/2017 06:24 | 1722 | 8 | 66 |
| Kohnen16-17_N_08 | 10/01/2017 06:40 | 11/01/2017 06:15 | 1890 | 6 | 45 |
| Kohnen16-17_N_09 | 11/01/2017 06:34 | 12/01/2017 06:22 | 1784 | 9 | 72 |
| Kohnen16-17_N_10 | 12/01/2017 06:39 | 13/01/2017 06:24 | 1724 | 13 | 106 |
| Kohnen16-17_N_11 | 13/01/2017 06:44 | 14/01/2017 06:26 | 1736 | 10 | 79 |
| Kohnen16-17_N_12 | 14/01/2017 06:47 | 15/01/2017 08:26 | 1811 | 8 | 67 |
| Kohnen16-17_N_13 | 15/01/2017 08:45 | 16/01/2017 06:25 | 1574 | 14 | 112 |
| Kohnen16-17_N_14 | 16/01/2017 06:44 | 17/01/2017 06:24 | 1754 | 8 | 63 |
| Kohnen16-17_N_15 | 17/01/2017 06:42 | 18/01/2017 06:17 | 1717 | 4 | 31 |
| Kohnen16-17_N_16 | 18/01/2017 06:34 | 19/01/2017 06:23 | 1392 | 5 | 38 |
| Kohnen16-17_N_17 | 19/01/2017 06:43 | 20/01/2017 06:23 | 1686 | 4 | 35 |
| Kohnen16-17_N_18 | 20/01/2017 06:47 | 21/01/2017 05:59 | 1742 | 5 | 36 |
| Kohnen16-17_N_19 | 21/01/2017 06:15 | 21/01/2017 09:36 | 256 | n.d. | n.d. |
| Kohnen16-17_N_20 | 21/01/2017 10:00 | 21/01/2017 13:34 | 286 | n.d. | n.d. |
| Kohnen16-17_N_21 | 21/01/2017 14:02 | 21/01/2017 17:44 | 267 | n.d. | n.d. |
| Kohnen_16-17_N_22 | 21/01/2017 18:05 | 21/01/2017 21:36 | 257 | n.d. | n.d. |
| Kohnen_16-17_N_23 | 21/01/2017 22:00 | 22/01/2017 01:35 | 256 | n.d. | n.d. |
| Kohnen_16-17_N_24 | 22/01/2017 02:00 | 22/01/2017 05:37 | 257 | n.d. | n.d. |
| Kohnen_16-17_N_25 | 22/01/2017 06:00 | 22/01/2017 09:34 | 256 | n.d. | n.d. |
| Kohnen_16-17_N_26 | 22/01/2017 10:00 | 22/01/2017 13:36 | 265 | n.d. | n.d. |
| Kohnen_16-17_N_27 | 22/01/2017 14:00 | 22/01/2017 17:38 | 268 | n.d. | n.d. |
| Kohnen_16-17_N_28 | 22/01/2017 18:00 | 22/01/2017 21:43 | 271 | n.d. | n.d. |
| Kohnen_16-17_N_29 | 22/01/2017 22:02 | 23/01/2017 01:43 | 268 | n.d. | n.d. |
| Kohnen_16-17_N_30 | 23/01/2017 02:05 | 23/01/2017 05:49 | 270 | n.d. | n.d. |
| Kohnen_16-17_N_31 | 23/01/2017 06:05 | 24/01/2017 06:22 | 1764 | 5 | 45 |
| Kohnen_16-17_N_32 | 24/01/2017 06:39 | 25/01/2017 07:56 | 1821 | 6 | 50 |

| | | | | | |
|---|---|---|---|---|---|
| Kohnen_16-17_N_33 | 25/01/2017 08:33 | 26/01/2017 06:07 | 1570 | 8 | 29 |
| Kohnen_16-17_N_34 | 26/01/2017 06:36 | 27/01/2017 06:07 | 1718 | 1 | 7 |
| Kohnen_16-17_N_35 | 27/01/2017 06:36 | 28/01/2017 06:07 | 1682 | 1 | 4 |

*STP: standard temperature and pressure.

## References


Erbland, J., Savarino, J., Morin, S., France, J., Frey, M., and King, M.: Air–snow transfer of nitrate on the East Antarctic Plateau–Part 2: An isotopic model for the interpretation of deep ice-core records, Atmospheric Chemistry and Physics, 15, 12079-12113, 2015.

Kukui, A., Loisil, R., Kerbrat, M., Frey, M., Gil Roca, J., Jourdain, B., Ancellet, G., Bekki, S., Legrand, M., and Preunkert, S.: OH and RO2 radicals at Dome C (East Antarctica): first observations and assessment of photochemical budget, EGU General Assembly Conference Abstracts, 2013.

Weller, R., and Wagenbach, D.: Year-round chemical aerosol records in continental Antarctica obtained by automatic samplings, Tellus B: Chemical and Physical Meteorology, 59, 755-765, 2007.